Ultra-high aspect ratio hybrid materials: The role of organic guest and synthesis method

G. V. Manohara, Li Li, Andrew Whiting and H. Chris Greenwell

Hybrid organic-inorganic layered double hydroxide materials have been prepared with an ultra-high aspect ratio via an environmentally friendly co-hydration approach where metal hydroxides and adamantane-carboxylic acid were used as the reagents. The method avoids use of either acidic or basic precipitation methods, or using a large excess of anion. The effect of organic anion, metal cation and synthesis method on developing ultra-high aspect ratio crystallites was studied.

Over the last two decades, nanocomposites comprising various functional materials have gained prominence over individual compounds/materials owing to their enhanced properties and their potential applications.[1] This has resulted in the displacement of conventional functional materials by hybrid nanocomposites in various fields including catalysis, sorption, energy, medicine, engineering and so on. Layered solids such as graphite and related materials,[2] cationic clays,[3] layered double hydroxides (LDHs),[4] dichalcoginides[5] and metal organic frameworks[6] have all been studied as filler particles for high performance hybrid nanocomposites. Among functional materials, LDHs show beneficial properties including photochemical activity, redox chemistry, anion exchange,[7] surface basicity[8] and reversible thermal behaviour.[9] In addition, these materials are, generally, environmentally benign, have readily varied composition and are economical to prepare.

Layered double hydroxides (LDHs), also known as anionic clays, are inverse charge analogues of cationic clays in their microstructure and properties.[10] The largest group of the LDH family of materials consists of positively charged metal hydroxide layers having the composition $[M^{II}_{1-x}M'^{III}_x(OH)_2]^{x+}$ (M^{II} = Mg, Ca, Co, Ni, Cu, Zn; M'^{III} = Al, Cr, Fe; $0.2 \leq x \leq 0.33$) with a brucite $(Mg(OH)_2)$-like structure. The positive charge on the sheets, imparted by isomorphous substitution of the M^{III} species, is balanced by the anions present in the interlayer region between

the sheets. This results in the general formula $[M^{II}_{1-x}M'^{III}_x(OH)_2](A^{n-})_{x/n}\cdot mH_2O$ (m = 0.33-0.50).[11]

LDHs are an increasingly studied class of layered solid materials owing to their utility, however much research is still required and directed at understanding: (a) ambiguity in LDH structure and property correlation; (b) challenges in synthesizing phase pure LDH materials; (c) the considerable composition variability of LDHs; and (d) the LDH structure being prone to various structural disorders.

The aspect ratio of the layered solid filler particles plays an important role in developing nanocomposite materials with optimal mechanical reinforcement and/or gas/vapour barrier properties. The aspect ratio of a solid is defined as the ratio of breadth of the layer to the thickness of the individual layer. The thickness of the single layer is the fixed value and it depends on the kind of layered solid, for example the thickness of a single LDH sheet is around 4.6 Å. The breadth of the layer mainly depends on the synthesis method and, to some extent, on the nature of the material as well.

Generally, LDHs crystallise with hexagonal platelet morphology, and assemble in aggregates having a particle size in the sub-micron range, with a particle basal breadth generally less than 1 μm and a layer aspect ratio in the order of 10-100. Within polymer nanocomposites, LDHs have the potential to be employed as oxygen barriers,[12] as reinforcing fillers,[13] as flame-retardants[14] and so on. For all these applications, high aspect ratio platelets that can be readily dispersed with various solvents to offer a variety of functional materials are preferred.

Hitherto, the synthesis of high aspect ratio LDH platelets having improved dispersion capability has been challenging.[15] The structure of the anion, the charge on the anion and the synthesis method have been shown to play a key role in realizing high aspect ratio LDHs. So far, only carbonate intercalated LDHs prepared by the homogeneous precipitation from solution (HPFS) method (by using urea/hexamethylenetetramine (HMT) as hydrolyzing agents) is known to give carbonate LDHs with high aspect crystal platelets.[16,17] Kayano and Ogawa studied the effect of reaction time and temperature on the final morphology of LDHs prepared by hydrolysis, and found lower temperatures and longer reaction times (100 days) resulted in the highest aspect ratio materials.[18] In order to make use of individual, well dispersed LDH sheets for various

applications one needs to be able to exfoliate/delaminate these layers in various solvents.[19-22] Since carbonate LDHs are thermodynamically very stable, and carbonate in minerals has a very low hydration enthalpy it is difficult to exchange it for other ions, or exfoliate LDHs containing it.[23] As a result, carbonate containing LDH materials have restricted usage. There are attempts to prepare high aspect ratio non-carbonated LDHs starting from the carbonate LDH.[24] However, this approach has multiple steps and is cumbersome. Recently, successful attempts were made to synthesize non-carbonated LDHs through the HPFS method, but the resultant crystallites had a rather low aspect ratio.[25] Kelkar and Schutz studied the crystal morphology of LDHs as a function of the type of organic anion and showed that the mono-valent organic acids promoted LDH crystal growth perpendicular to the c crystallographic axis and higher aspect ratios, whereas dicarboxylic acids promoted growth parallel to the c axis.[26] However, these organic acids have not been exhaustively explored to realize high aspect ratio LDHs.

Herewith, we report the synthesis of high aspect ratio non-carbonate LDHs by employing a green synthesis method where metal hydroxides are used as precursors in a one-pot procedure.[27] The use of metal hydroxides,[28,29] or oxides,[30-32] as a LDH precursor has been studied from a green chemistry perspective, as often the synthesis pathway occurs at near neutral pH and allows a lower excess of the desired interlayer anion to be used than co-precipitation methods owing to the lack of competing carbonate anions in the reaction solution, problematic at high pH. As discussed above, the anion plays a critical role in mediating the growth and stacking of the metal hydroxide sheets. The adamantane moiety is the first member of the diamondoid family and has T_d symmetry and is highly hydrophobic.[33] The spatial arrangement of the carbon atoms in adamantane is similar to that seen in the extended diamond structure. Adamantane carboxylic acid is a functional derivative of adamantane and was used as the anion in our synthesis with the objective to mediate the growth of high aspect ratio LDHs through utilising the highly hydrophobic and mono-anionic nature of the adamantane moiety to promote LDH growth perpendicular to the c crystal axis.

In a typical experiment, a stoichiometric amount of $M(OH)_2$ [M= Mg^{2+} and Ca^{2+}], $Al(OH)_3$ and 1-adamantane-carboxylic acid (ACA) was added to 50 mL of deionized water and stirred at room temperature for an hour [M^{2+}/Al^{3+}= 2, ACA/Al^{3+} =1]. Subsequently, the resultant reaction mixture was hydrothermally treated at 150 °C for 24 h in a Parr stirred autoclave. Since the metal

hydroxides were used as precursors, and a stoichiometric amount of 1-adamantane-carboxylic acid was used, the sample was recovered by centrifugation without involving any post synthesis washing to remove excess salts or anions. To check the influence of the synthesis method on the resultant crystallite size, Mg-Al LDH with adamanatane-carboxylate was also synthesized by employing the typically used co-precipitation method, starting with soluble metal nitrates as precursors, and at pH 10. Three times the stoichiometric requirement of adamanatane-carboxylate was used (as the sodium salt) to prepare the LDH. The co-precipitation was carried out at 65 °C, under a nitrogen atmosphere to preclude the formation of the competing carbonate anion from atmospheric CO_2 in the high pH suspension. The product was recovered by centrifugation followed by washing with copious amounts of water. Hot deionized water was used throughout the synthesis to further avoid the potential for carbonate anion contamination.

Figure 1a shows the PXRD pattern of Mg-Al-adamantane-carboxylate LDH and shows the basal reflection (*001*) at 20.64 Å (4.28 2° 2θ) corresponds to a bilayer arrangement of adamantane ions in the interlayer (based on an anion length, along its principle axis or rotational symmetry, of 7.0 Å).[34] The sub-multiples of the (*001*) reflections are seen at 10.2 Å (8.67), 6.78 Å (13.05) and 4.04 Å (21.95 2° 2θ). The observed *d*-spacing of the adamantane-carboxylate intercalated LDH matches with the reported value for similar adamantane LDHs prepared by anion exchange and reconstruction/memory effect methods (and thus with crystal size representing the original co-precipitated material).[35,36] Intercalation of adamantane-carboxylate into the interlayer galleries of the Mg-Al LDH was further characterized with IR spectroscopy (Figure 2a). The vibrations at 1517 cm^{-1} and 1397 cm^{-1} correspond to anti-symmetric and symmetric stretching vibrations of the COO$^-$ group and vibration at 2904 cm^{-1} and 2849 cm^{-1} are for the C-H vibrations of the adamantane-carboxylate ion.[37] The 3400 cm^{-1} vibration is due to hydrogen bonding of the layer metal hydroxide groups with intercalated water molecules in the interlayer. These vibrations further confirm the successful intercalation of adamantane-carboxylate. The intercalated adamantane-carboxylate was also characterized by ^{1}H and ^{13}C solid-state NMR. The ^{1}H NMR spectra of the sample (Figure 3) shows a sharp peak at 1.01 ppm corresponding to the CH$_2$ protons of the adamantane ring and a broad peak centered around 1.74 ppm, which is due to CH protons of the adamantane ring. The other two peaks at 3.80 and 4.69 ppm are due to the protons of the intercalated water in the interlayer region, and the hydroxyls in the metal hydroxide layer, respectively. The ^{13}C NMR spectra of Mg-Al-adamantane-carboxylate (Figure 4) shows 4 sharp

peaks in the low field region at 29.5, 37.3, 40.6 and 42.8 ppm, due to 4 different carbon environments present in the adamantane molecule. The peak at 187.0 ppm is due to the carbon atom of the carboxylate group.

The thermal behavior of the Mg-Al-adamantane-carboxylate LDH was studied by thermogravimetric analysis (TGA) under an N_2 atmosphere, from room temperature up to 800 °C and results are given in Figure 5a. Overall, the LDH loses up to 70% mass owing to the higher mass content of the intercalated adamantane carboxylate ion, water and dihydroxylation of the hydroxide layers. Interestingly, the LDH shows higher thermal stability up to around 550 °C. Generally, LDHs lose intercalated anions and layered hydroxyls at below temperatures of *circa* 400 °C, leading to the formation of mixed metal oxides.[38] However, in the present case, the higher thermal stability may be explained based on the thermal stability of the intercalated adamantane-carboxylate ion. Elemental analysis of the Mg-Al-adamantane-carboxylate LDH gave 30.35 %C and 5.53 %H. The LDH-adamantane samples were extremely hydrophobic and problematic to dissolve in mineral acids to analyse the metal content; as such X-ray fluorescence (XRF) spectroscopy was used to determine the Mg/Al ratio to be 2.11. Using this Mg/Al ratio, a calculated formula of $[Mg_{0.68}Al_{0.32}(OH)_2]Ada_{0.32}.1.20H_2O$ can be derived, if we assume that adamantane is the only anion. This then gives a theoretical 30.62 %C, 5.19 %H, 41.77 % mass of adamantane-carboxylate and 15.56 % structural water (mass loss < 200 °C in TGA), which is in good agreement to the elemental analysis and TGA, but appears to slightly overestimate the water content (12 % in the TGA). There was also good agreement between calculated and observed residual mass (29.68 % and *ca* 30 %, respectively).

Electron microscope (EM) images of the synthesized Mg/Al-adamantane-carboxylate LDHs show platelet morphology, typical of layered materials with high aspect ratio as evident in the scanning EM (SEM) image in Figure 6a. The crystallites have a breadth of the basal planes as high as 20 μm and with an average size, by visual observation, of around 10 μm. Having a LDH layer thickness of 4.6 Å, adamantane-carboxylate LDHs have potential to generate hydroxide sheets having aspect ratios of circa 10,000 upon exfoliation. The small crystals present along with the larger platelets are likely due to broken edges. This is evident from the different magnification SEM images of the same sample as shown in the Figure SI 1 (in the ESI). When examined by transmission EM (TEM), shown in Figure 6b, the high aspect ratio of the dispersed

crystals is clear, where edges are folded over it can be seen that the thickness of the crystal along the c axes is less than 5 nm, and possibly as low as 2 nm, corresponding to the basal spacing identified by XRD and suggestive of single LDH sheets. This is confirmed by high resolution TEM (Figure 6c), where an upturned edge shows a crystal thickness of around 10 nm, with several layers showing.

The growth of these large crystals can be accounted for through the combination of intercalated anion used, and the synthesis method. To verify this, we synthesized Mg-Al-adamantane-carboxylate intercalated (Mg/Al=2) LDH by co-precipitation at pH 10. Figure 1c shows the PXRD pattern of the co-precipitated LDH, which shows the d-spacing of 20.45 Å (4.32 2° 2θ). The sub-multiples of this can be seen at 9.68 Å (9.13) and 6.41 Å (13.08 2° 2θ). The d-spacing of the co-precipitated sample is a little lower than the hydrothermally synthesized sample. This could be on account of different degree of hydration, or inclusion of the anion in the interlayer. The IR spectrum of the sample (Figure 2c) shows 3396, 2899, 2853, 1522 and 1391 cm^{-1} vibrations, matching with those of the hydrothermally prepared sample. The TGA thermogram of the sample is shown in the Figure 5b and shows similar characteristics to those observed in the hydrothermally prepared sample. The SEM images of the co-precipitated sample are given in the figures in SI 2, and shows aggregated particles with submicron size. This is a typical morphology expected from the co-precipitation method. As co-precipitation does not result in high aspect ratio crystals, this clearly shows the concerted role of the precursors, the anion and type of synthesis method in developing high aspect ratio LDH crystals.

Encouraged with the results for Mg-Al LDH system, a synthesis of Ca-Al LDH was attempted in a similar way. Ca-Al LDHs are the subject of relatively fewer studies, when compared to the Mg-Al system due the complexity involved in the synthesis of these materials.[39] In LDHs, the larger ionic radii Ca^{2+} has coordination number of 7, which is not compatible with the octahedral environment of the commonly encountered layered double hydroxide (hydrotalcite-like) mineral structures. This adds to the complexity of realising phase pure Ca-containing LDHs.[40] Additionally, other phases of the Ca system, namely CaCO$_3$, are thermodynamically more stable than the hydroxide and as a result, it is difficult to synthesize phase pure Ca-Al LDH. However, Ca-Al LDH is more basic and economical compared to the Mg-Al system. Therefore, it is of interest to prepare high aspect ratio Ca-Al LDHs. Similar to the Mg-Al system, Ca-Al-

adamantane-carboxylate was synthesized starting with $Ca(OH)_2$, $Al(OH)_3$ (Ca/Al=2) and 1-adamantane-carboxylic acid (ACA/Al^{3+} =1) by employing a hydrothermal method at 150 °C.

The PXRD pattern of Ca-Al-adamantane carboxylate is given in Figure 1b and shows the first three basal reflections at 20.31 Å (4.35), 10.16 Å (8.70) and 6.72 Å (13.17 2° 2θ) respectively. The *d*-spacing of 20.31 Å, for Ca-Al system is somewhat smaller than Mg-Al LDH and this could again be due to different degree of hydration in the interlayer. Interestingly, the crystallinity of Ca-Al LDH is much better than the Mg-Al LDH system, as evident from the intensity of the reflections in the PXRD patterns in Figure 1. The intercalation of adamantane carboxylate ion into the interlayer space was further characterized by IR spectroscopy, as shown in Figure 2b. The symmetric and anti-symmetric carboxylate stretching vibrations are seen at 1525 and 1400 cm^{-1}, respectively. The C-H vibrations, along with hydroxyl stretching, are seen at 2909/2853 and 3387 cm^{-1}, respectively.

The SEM images of the resultant Ca-Al LDH (Figure 6d) showed crystallites having breadth ranging from 3 to 20 μm and clearly of lower aspect ratio, with more layers per crystallite wen compared to the Mg-Al LDH in Figure 6a. It can also be observed that the crystallite sizes were not uniform when compared to the Mg-Al system. Owing to beam damage of the LDHs in the SEM, and the presence of the insulating adamantane carboxylate ion in the interlayer, it was challenging to undertake a high resolution SEM study of the morphology of the resultant LDHs (SI. 3). However, TEM imaging (Figure 6e) clearly shows the hexaplaty nature of the crystals. HR-TEM analysis, exemplified in Figure 6f, shows an usual corrugated/wrinkled morphology, which may be owing to the distortion that is known to exist in such materials owing to the 7-coordinate nature of the larger Ca^{2+} cation.

The thermal behavior of the Ca-Al LDH was studied by TGA, as shown in Figure 5c. Both the PXRD and IR data of the Ca-Al-adamantane-carboxylate LDH shows successful formation of the LDH. Elemental analysis yielded a composition of 31.08 %C and 4.92 %H, while XRF analysis gave a Ca/Al molar ratio of 1.78. Based on the experimental Ca/Al ratio, and assuming minimal carbonate contamination, a calculated formula of [$Ca_{0.64}Al_{0.36}(OH)_2$]$Ada_{0.36}$.$1.05H_2O$ gives 30.90 %C, 5.09 %H, 42.16 % mass of adamantane-carboxylate and 12.39 % structural water (mass loss < 200 °C in TGA). This is in good agreement with both the experimental and TGA data, but, compared to the TGA data (*ca* 15 % mass loss < 200 °C) underestimates the

water incorporated and the total residual mass (33.67 % calculated, *ca* 38 % observed). There is a difference in the initial water loss curve between the two materials, with the Ca-Al LDH losing water rapidly relative to the Mg-Al LDH.

In conclusion, we show that we have been able to use a highly hydrophobic modifier, adamanatane-carboxylic acid, coupled to hydrothermal synthesis conditions to prepare LDH particles of unusually high aspect ratio. These materials are especially promising for applications in composite materials or as rheology modifiers in oil based fluids and future work will continue to probe the thermal stability of these materials as well as their applications.

Notes and references

1. B. Chen, J. R. G. Evans, H. C. Greenwell, P. Boulet, P. V. Coveney, A. A. Bowden, A. Whiting. *Chem. Soc. Rev.,* 2008, **37**, 568.

2. O. C. Compton, S. T. Nguyen. *Small.*, 2010, **6**, 711.

3. M. Alexandre, P. Dubois. *Materials Science and Engineering.*, 2000, **28**, 1.

4. M. Q. Zhao, Q. Zhang, J. Q. Huang, F. Wei. *Adv. Funct. Mater.*, 2012, **22**, 675.

5. T. Stephenson,Z. Li, B. Olsen, D. Mitlin. *Energy Environ. Sci.*, 2014, **7**, 209.

6. (a) C. Sanchez, B. Julian, P. Belleville, M. Popall. *J. Mater. Chem.*, 2005, 15, 3559; (b) C. Petit, T. J. Bandosz. *Adv. Mater.*, 2009, **21**, 4753.

7. M. Meyn, K. Beneke, G. Lagaly. *Inorg. Chem.*, 1990, **29**, 5201.

8. W. T. Reichle. *J. Catal.*, 1985, **94**, 574.

9. S. Miyata. *Clays Clay Miner.*, 1980, **28**, 50.

10. F. Cavani, F. Trifiro, A. Vaccari. *Catal. Today.*,1991, **11**, 173.

11. X. Duan, D. G. Evans. Layered double hydroxides, in: D. M. P. Mingos (Ed.), Struct. Bonding, Springer-Verlag, Berlin Heidelberg, 2006, pp. 1-233.

12. Y. Dou, S. Xu, X. Liu, J. Han, H. Yan, M. Wie, D. G. Evans, X. Duan. *Adv. Funct. Mater.*, 2014, **24**, 514.

13. F. Leroux, J. P. Besse. *Chem. Mater.*, 2001, **13**, 3507.

14. (a) Y. Gao, J. Wu, Q. Wang, C. A. Wilkie, D. O'Hare. *J. Mater. Chem. A.*, 2014, **2**, 10996; (b) Z. Matusinovic, C. A. Wilkie. *J. Mater. Chem.*, 2012, **22**, 18701.

15. U. Costantino, F. Marmottini, M. Nocchetti, R. Vivani. *Eur. J. Inorg. Chem.*, 1998, **10,** 1439.

16. Q. Wang, D. O'Hare. *Chem. Commun.*, 2013, **49**, 6301.

17. N. Iyi, T. Matsumoto, Y, Kaneko, K. Kitamura. *Chem. Lett.*, 2004, **33**, 1122.

18. M. Kayano, M. Ogawa, *Clays Clay Miner.*, 2006, **54**, 382.

19. T. Hibino, *Chem. Mater.*, 2004, **16**, 5482.

20. N. Iyi, Y. Ebina, T. Sasaki, *Langmuir.*, 2008, **24**, 5591.

21. Z.Liu, M.Renzhi, Y.Ebina, N. Iyi, K.Takada, T.Sasaki, *Langmuir.*, 2007, **23**, 861.

22. M. Khaldi, A. De Roy, M. Chaouch, J. P. Besse. *J. Solid State. Chem.*, 1997, **130**, 66.

23. R. K. Allada, J. D. Pless, T. M. Nenoff, A. Navrotsky. *Chem. Mater.*, 2005, 17, 2455.

24. N. Iyi, T. Matsumoto, Y. Kaneko, K. Kitamura. *Chem. Mater.*, 2004, **16**, 2926.

25. C. A. Anthonyraj, P. Koilraj, S. Kannan. *Chem. Commun.*, 2010, **46**, 1902.

26. (a) M. A. Drezdon. *Inorg. Chem.*, 1988, **27**, 4628; (b) C. P. Kelkar, A. A. Schutz. *Microporous Mater.*, 1997, **10**, 163.

27. (a) M. Ogawa, S. Asai. *Chem. Mater.* 2000, **12**, 3253; (b) H. C. Greenwell, W. Jones, S. L. Rugen-Hankey, P. J. Holliman, R. L. Thompson. *Green Chem.*, 2010, **12**, 688.

28. M. Ogawa, F. Saito, *Chem. Lett.*, 2004, 1030.

29. M. Ogawa, Y. Sugiyama, *J. Ceram. Soc. Jpn.*, 2009, **117**, 179.

30. S. Newman, W. Jones, P. O'Connor, D. N. Stamires., *J. Mater. Chem.*, 2002, **12**, 153.

31. Z. P. Xu, G. Q. Ku, *Chem. Mater.*, 2005, **17**, 1055.

32. H. C. Greenwell, C. C. Marsden, W. Jones, *Green Chem.*, 2007, **9**, 1299.

33. (a) J. E. Dahl, S. G. Liu, R. M. K. Carlson. *Science.*, 2003, **299**, 96 ; (b) H. Schwertfeger, A. A. Fokin, P. R. Schreiner. *Angew. Chem. Int. Ed.,* 2008, **47**, 1022.

34. F. Belanger-Gariepy, F. Brisse, P. D . Harvey, D. F. R. Gilson, I. S. Butler. *Can. J. Chem.*, 1990, **68**, 1163.

35. A. I. Khan, G. R. Williams, G. Hu, N. H. Rees, D. O'Hare. *J. Solid State Chem.,* 2010, 183, 2877.

36. U. Costantino, F. Montanari, M. Nocchetti, F. Canepa, A. Frache. *J. Mater. Chem.,* 2007, **17**, 1079.

37. K. Nakamota, Infrared and Raman spectroscopy of inorganic and coordination compounds, Wiley, New York, 1986.

38. V. Rives, Layered Double Hydroxide: Present and Future, Ed. V. Rives, Nova Science Publisher. Inc, New York, 2006, Chapter 4, 127-151.

39. M. Yang, E. Tuckley, J.C. Buffet, D. O'Hare. *J. Mater. Chem. A.*, 2016, **4**, 500.

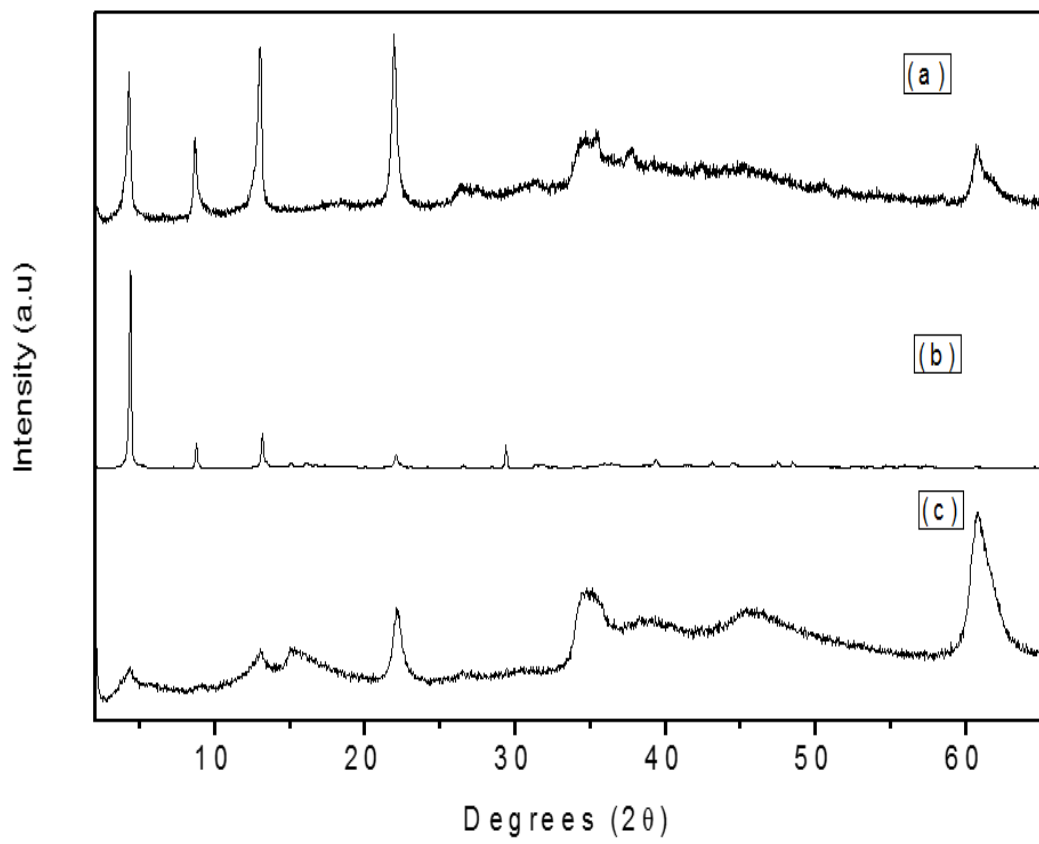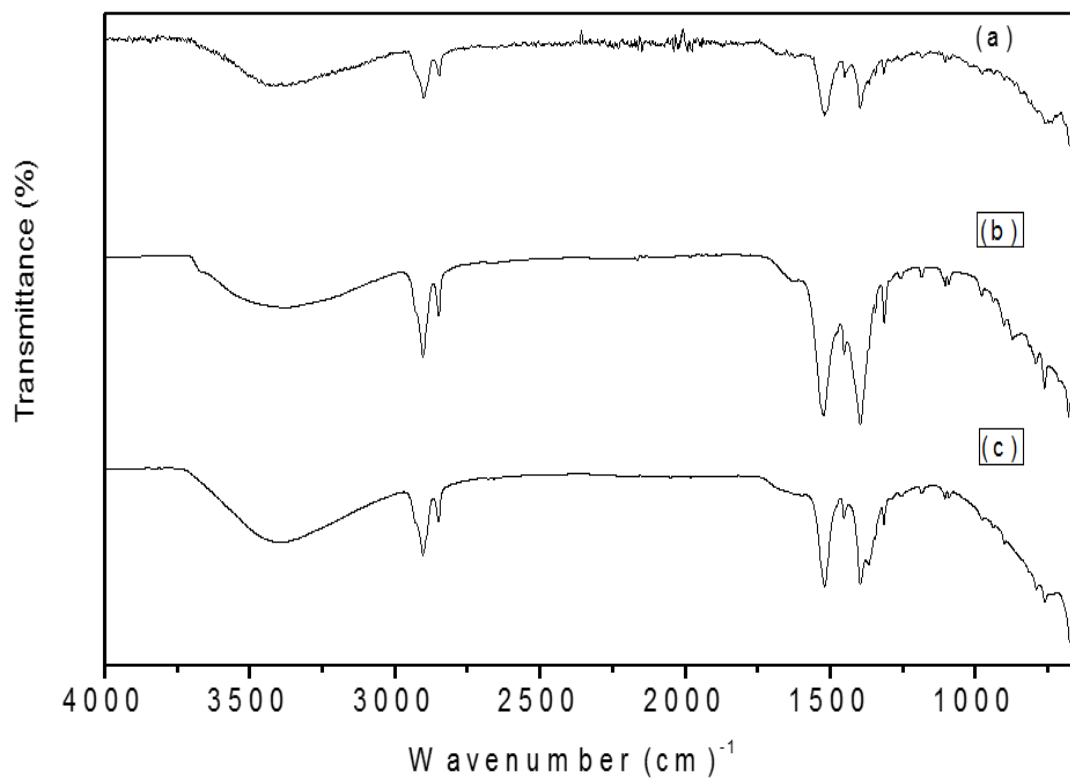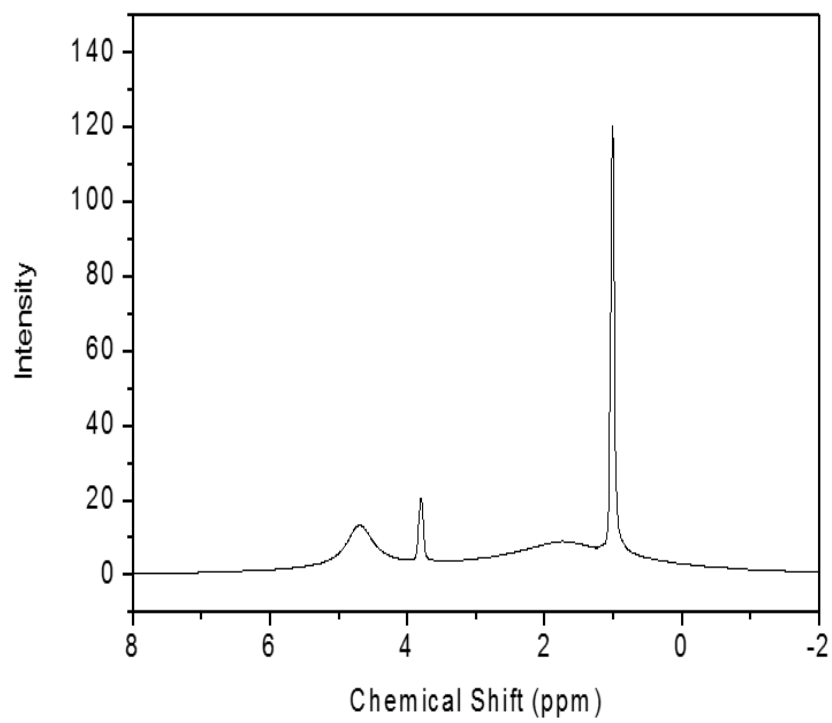40. A. G. Kalinchev, R. J. Kirkpatrick, R. T. Cygan. *American. Miner.*, 2000, **85**, 1046.
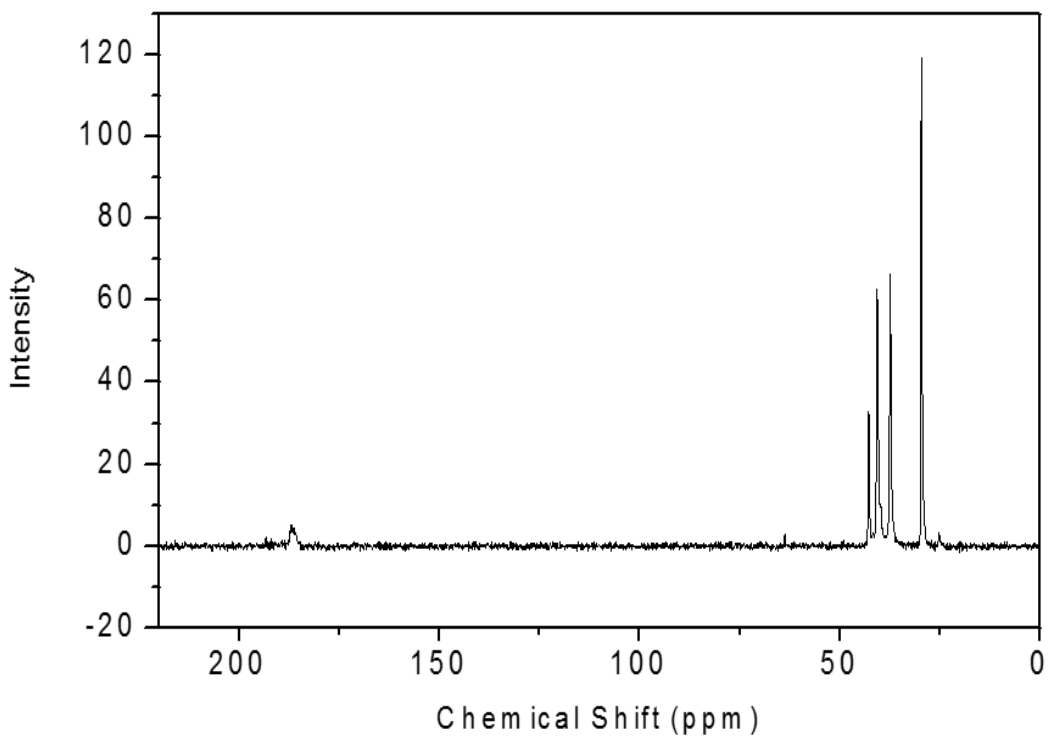
Figure 1

Figure 2

Figure 3

Figure 4

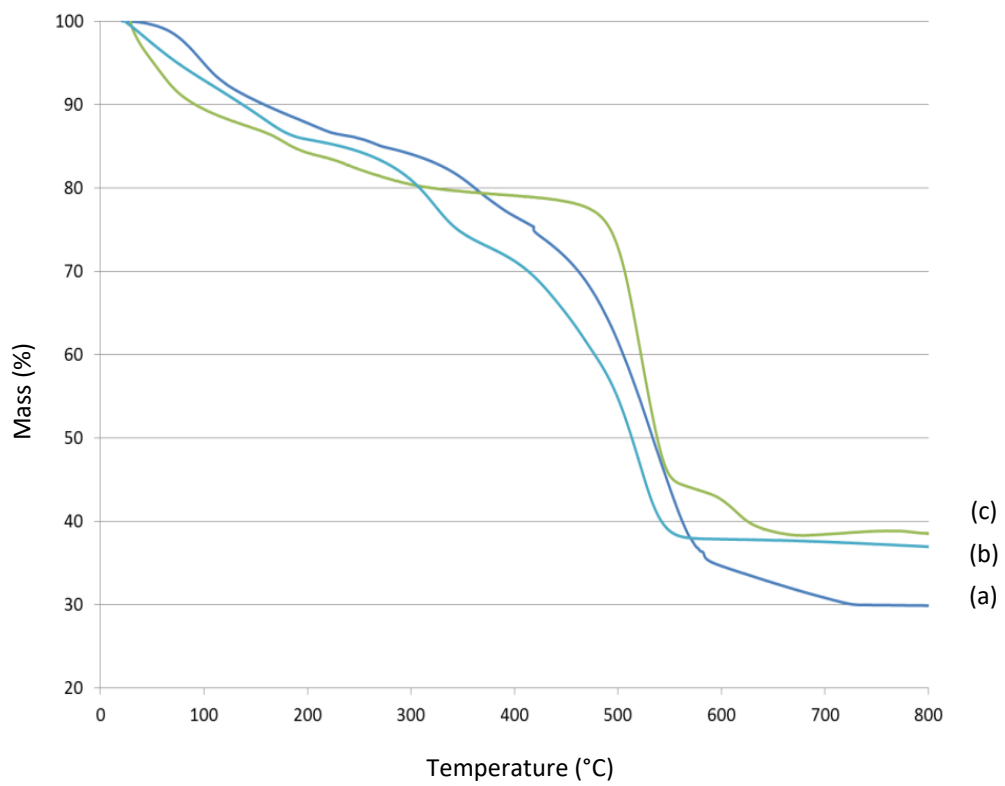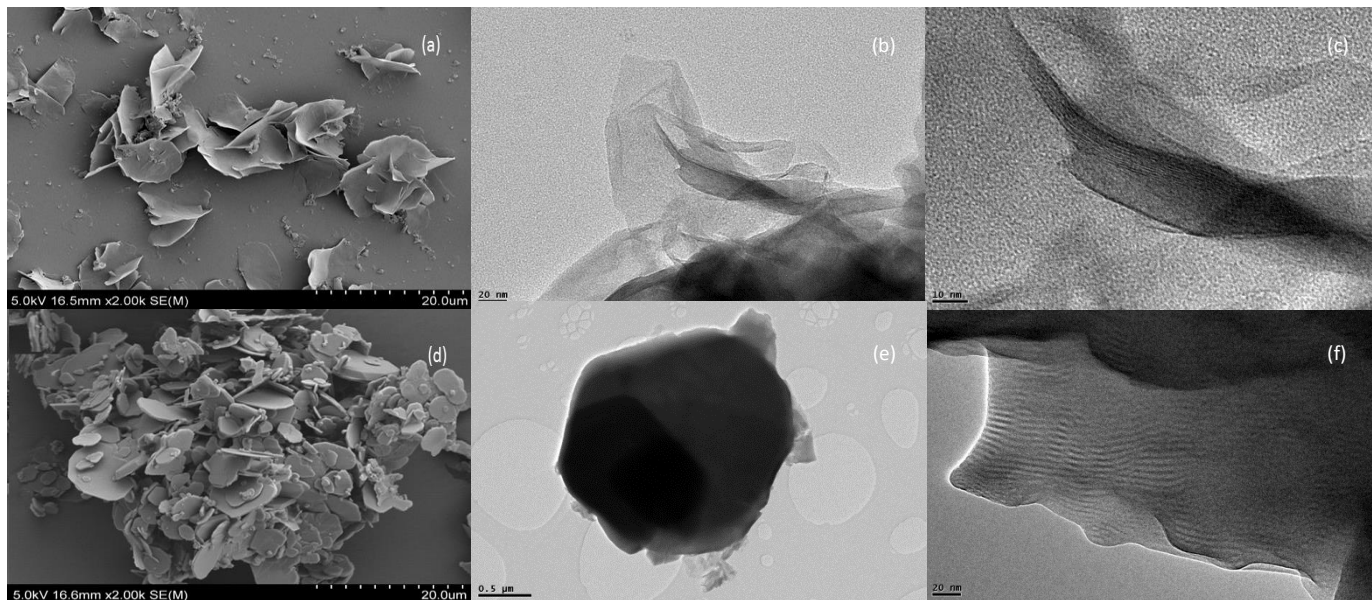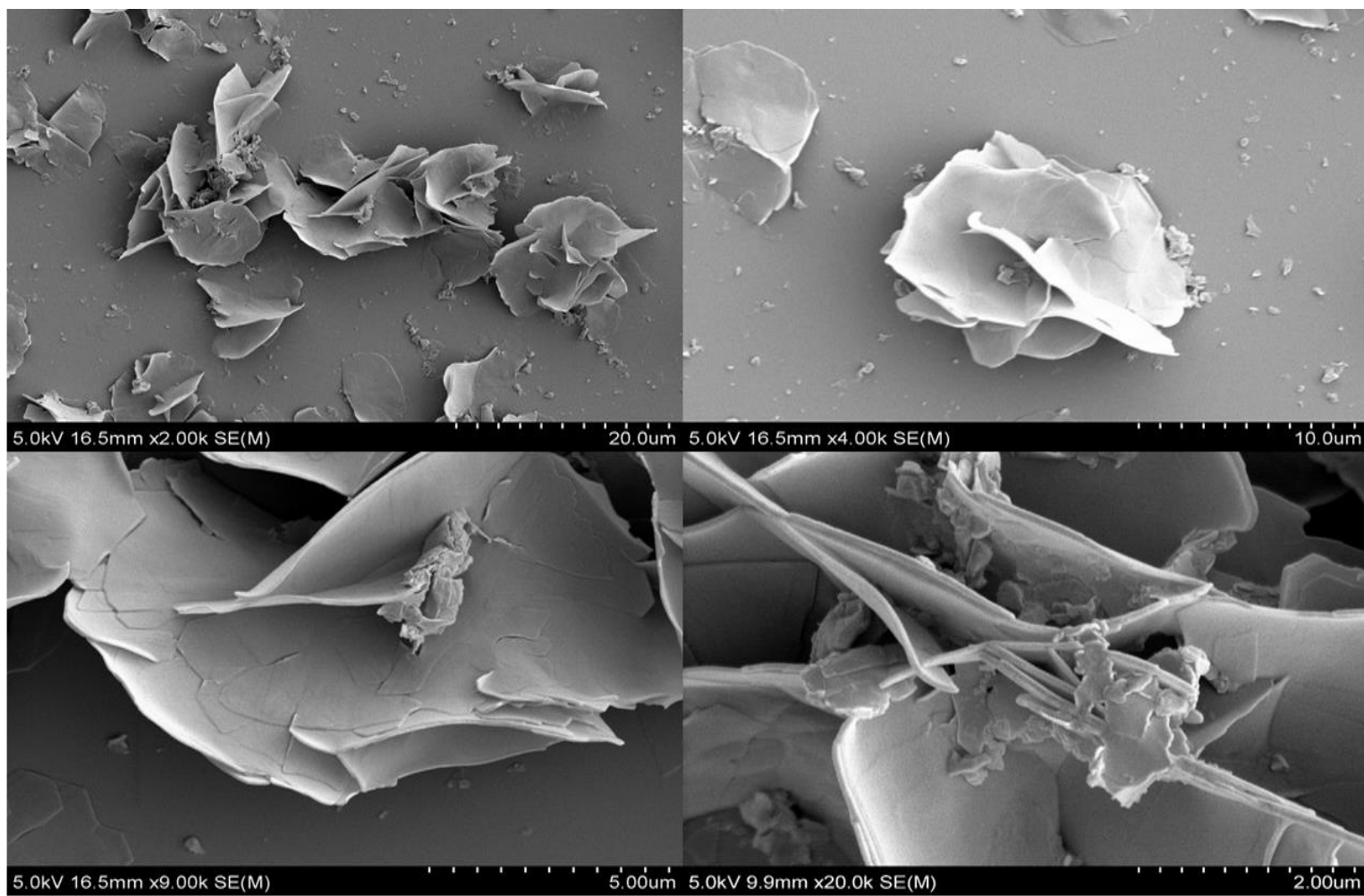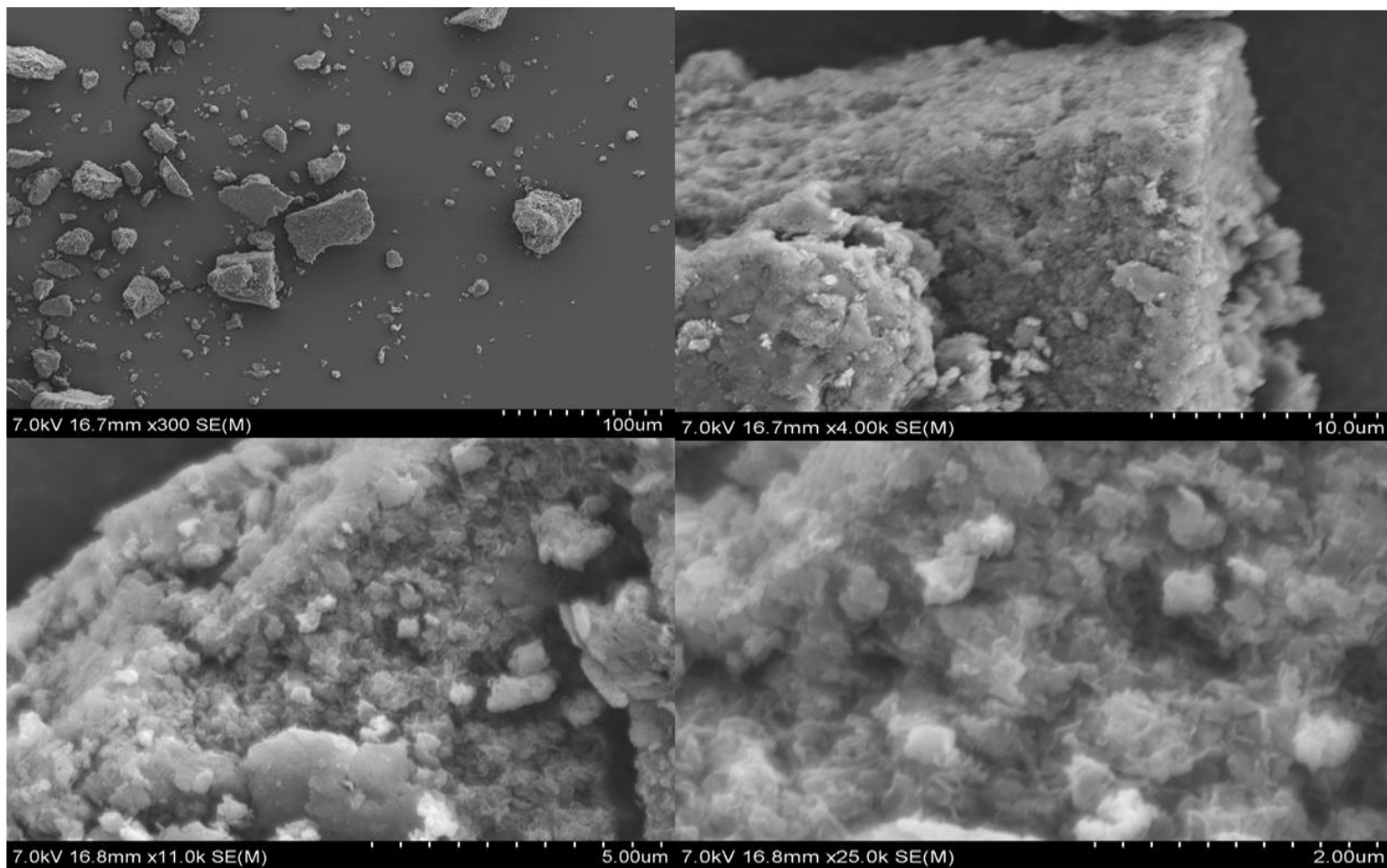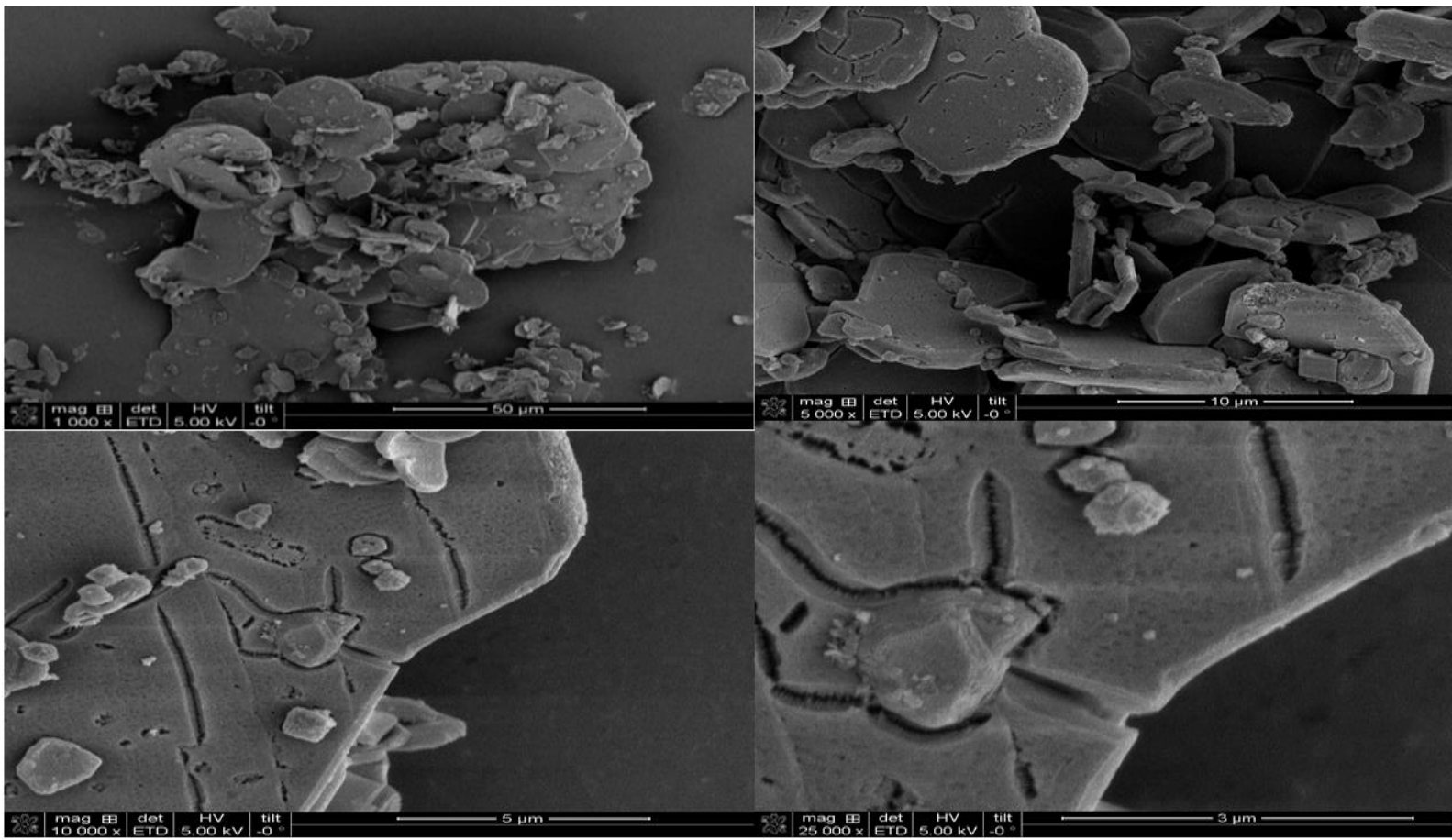Figure 5

Figure 6

SI. 1 SEM images of Mg-Al-adamantanecarboxylate intercalated LDH (Mg/Al=2).

SI. 2 SEM images of Mg-Al-adamantanecarboxylate LDH (Mg/Al=2) prepared by co-precipitation method at pH 10.

SI. 3 SEM images of Ca-Al-adamantanecarboxylate intercalated LDH (Ca/Al=2).

Figure Captions

Figure 1. PXRD pattern of adamantane-carboxylate intercalated LDHs: (a) Mg-Al (Mg/Al= 2) via hydroxide precursor route; (b) Ca-Al (Ca/Al= 2) via hydroxide precursor route; (c) Mg-Al (Mg/Al=2) prepared by co-precipitation at pH 10.

Figure 2. IR spectra of adamantane-carboxylate intercalated LDHs: (a) Mg-Al (Mg/Al= 2) via hydroxide precursor route; (b) Ca-Al (Ca/Al= 2) via hydroxide precursor route; (c) Mg-Al (Mg/Al=2) prepared by co-precipitation at pH 10.

Figure 3. Solid state ^{1}H NMR spectra of Mg-Al-adamantane-carboxylate LDH (Mg/Al=2) prepared by a hydroxide precursor route.

Figure 4. Solid state ^{13}C NMR spectra of Mg-Al-adamantane-carboxylate LDH (Mg/Al=2) by hydroxide route.

Figure 5. TGA profile of adamantane-carboxylate intercalated LDHs: (a) Mg-Al (Mg/Al= 2) prepared by the hydroxide precursor route; (b) Mg-Al (Mg/Al=2) prepared by co-precipitation at pH 10; (c) Ca-Al (Ca/Al= 2) LDH prepared by the hydroxide precursor route.

Figure 6. Electron microscopy images of adamantane-carboxylate LDHs prepared by the hydroxide precursor route for Mg-Al (Mg/Al=2): (a) SEM, (b) TEM, (c) HR-TEM and for Ca-Al (Ca/Al=2): (d) SEM, (e) TEM, (f) HR-TEM, showing the high aspect ratio and corrugated nature of the Ca-Al LDH.

SI. 1 SEM images of Mg-Al-adamantane-carboxylate intercalated LDH (Mg/Al =2).

SI. 2 SEM images of Mg-Al-adamantane-carboxylate LDH (Mg/Al=2) prepared by co-precipitation method at pH 10.

SI. 3 SEM images of Ca-Al-adamantane-carboxylate intercalated LDH (Ca/Al=2).

Characterization

Powder X-ray diffraction (PXRD) data was collected using a Bruker D8 Advance diffractometer (θ-2θ scan, Cu Kα radiation, λ = 1.541 Å). Data was collected at a continuous scan rate of 2 °2θ min^{-1} between 2 and 70 °2θ. Samples were gently ground powders, pressed into sample holders.

Infrared (IR) spectroscopy analyses of the samples were recorded in reflectance mode using a Perkin Elmer Spectrum 100 FT-IR spectrometer in attenuated total reflectance (ATR) mode. Ground powder samples of the LDH materials were used.

Thermogravimetric analysis (TGA). Each thermal analysis of the samples was carried out under a N_2 atmosphere using a TA 500 thermal analyzer. Approximately 20 mg of each ground powder sample was used. Each sample was heated from room temperature to 800 °C at a ramp rate of 30 °C.min^{-1} under a N_2 atmosphere.

Elemental analysis (CHN). C, H and N analysis on the LDH samples was carried out by the Microanalysis service within the Chemistry Department, Durham University. Approximately 3 mg of sample was placed in a tin capsule and combusted in a high oxygen environment at 950 °C using an Exeter Analytical CE-440 elemental analyser calibrated with acetanilide.

Solid state nuclear magnetic resonance (NMR) studies of the intercalated adamantine carboxylate ions (^{1}H and ^{13}C) were carried out using a Varian VNMRS spectrometer in the Solid State NMR facility, at the Department of Chemistry, Durham University.

Electron microscopy. Transmission electron microscopy (TEM), high resolution TEM (HR-TEM) and scanning electron microscopy (SEM) were carried out at the G. J. Russell Electron Microscopy facility, Department of Physics, Durham University. The surface morphology of all the samples were characterised using SEM, with all images obtained with a Hitachi SU-70 FEG SEM, except for the Ca-Al-adamantane carboxylate, given in SI. 3, which was recorded using a FEI Quanta 3D FEG SEM. The TEM and HR-TEM imaging was undertaken using a JEOL 2100F FEG TEM.

X-ray fluorescence (XRF) spectroscopy. The samples were provided as homogenized powders and weighed on a .1mg balance. The samples (93.8 mg and 26.7 mg) were placed directly into a Pt 95%/Au 5% crucible. To this, a lithium borate flux was added until the total weight of each sample and flux was 6.6 g. Claisse brand high purity flux was used containing 66.67% $Li_2B_4O_7$ – 32.83% $LiBO_2$ – and 5.0% LiI (releasing agent). The sample and flux were then mixed together using a wooden stirring implement, and placed in a Claisse La Neo Fluxer using the 'Refractory Materials' fixed conditions. The mixture was brought to a temperature of 1065 °C and rocked during fluxing. Total fluxing time was 15 min and the cooling time was 6 min. The fused beads were run on a Panalytical Zeitium WD-XRF with a 4 kW rhodium anode tube. The samples were analysed using the Panalytical proprietary 'Wroxi' calibration and corrections were made for the variable weight of each sample. The analysis time for each sample was 340 s.